

# Quasinormal modes of a charged loop quantum black hole

Li-Gang Zhu<sup>1,\*</sup>, Guoyang Fu<sup>2,†</sup>, Shulan Li<sup>3,‡</sup>, Dan Zhang<sup>1,§</sup> and Jian-Pin Wu<sup>1,¶</sup>

<sup>1</sup> *Center for Gravitation and Cosmology,  
College of Physical Science and Technology,  
Yangzhou University, Yangzhou 225009, China*

<sup>2</sup> *Department of Physics and Astronomy,  
Shanghai Jiao Tong University, Shanghai 200240, China*

<sup>3</sup> *Department of Physics, Shanghai University, Shanghai 200444, China*

## Abstract

This paper systematically investigates the quasinormal modes (QNMs) of a scalar field around a charged loop quantum black hole (BH). The BH is characterized by two key parameters: the quantum parameter  $b_0$  and the charge parameter  $Q$ . We explore two scenarios: one where the multipole quantum number  $l = 0$ , in which only the gravitational potential is relevant, and another where  $l > 0$ . For  $l = 0$ , quantum gravity effects lead to a pronounced overtone outburst in the quasinormal frequencies (QNFs), with the outburst and accompanying oscillatory patterns becoming more pronounced as the overtone number increases. For  $l > 0$ , the overtone outburst disappears due to the suppression of the quantum gravity effect by the centrifugal potential. However, a non-monotonic behavior in the first two overtones with respect to  $b_0$  is observed, indicating that subtle quantum gravity effects persist. This behavior vanishes as  $Q$  increases, further confirming the suppressive influence of the centrifugal potential on the quantum gravity effect.

---

\*zlgoupao@163.com

†FuguoyangEDU@163.com

‡shulanli.yzu@gmail.com

§danzhanglnk@163.com

¶jianpinwu@yzu.edu.cn

## Contents

<b>I. Introduction</b>	2
<b>II. Scalar field over the charged ABBV black hole</b>	5
<b>III. Quasinormal modes</b>	8
A. Fundamental modes	10
B. Overtones	12
C. QNFs with $l = 1$	14
<b>IV. Conclusions and discussions</b>	15
<b>Acknowledgments</b>	16
<b>References</b>	16

## I. INTRODUCTION

Loop quantum gravity (LQG) is considered a promising contender for the theory of quantum gravity, characterized by its non-perturbative and background-independent nature [1–4]. The quantization technique developed in full LQG has been effectively employed in the symmetry reduced cosmological model, resulting in the development of loop quantum cosmology (LQC) [5–12]. An outstanding characteristic of LQC is its ability to naturally substitute the classical big bang singularity of the universe with a quantum bounce [5–18], leading to a non-singular evolution of the universe [19, 20].

The approach developed in LQC can be readily applied to the spherically symmetric Schwarzschild black hole (BH) model, thereby opening up the field of loop quantum gravity black hole (LQG-BH). For a detailed construction of the model, please refer to [21–23] and also see the reviews [24, 25]. Just as LQC can address the Big Bang singularity of the universe, the LQG-BH model can likewise resolve the interior singularity of BHs. Specifically, for the majority of LQG-BHs, the singularity is substituted with a transition surface that connects a trapped region and an anti-trapped region.

Contrary to the LQC, which usually has a consistent treatment for various models, within

the framework of the LQG-BH model, there are various models that employ different schemes to regularize and quantize the Hamiltonian constraint. In general, the LQG-BH models can be categorized into three main schemes: the  $\mu_0$ -scheme, the  $\bar{\mu}$ -scheme, and the generalized  $\mu_0$ -scheme. In the  $\mu_0$ -scheme, it is assumed that the quantum regularization parameters remain constant over the whole phase space [21, 26–29]. An inherent drawback of this approach is that the final outcome is dependent on the fiducial structures introduced in the construction of the classical phase space. In addition, even in situations with low curvature, notable quantum effects may emerge, rendering these models non-physical. To eliminate the dependency on fiducial structures, the  $\bar{\mu}$ -scheme is proposed, in which the quantum regularization parameters are selected as a function of the phase space variables [22, 23, 30, 31]. In particular, in this scheme with Chou’s choice [23, 31], the spacetime rapidly converges to the Schwarzschild geometry when the curvatures are low, which addresses the disadvantage of the  $\mu_0$ -scheme [32–35]. Nevertheless, the  $\bar{\mu}$ -scheme is also subject to the drawback that the quantum corrections to the Schwarzschild BH horizon may be substantial, contrary to the prevailing belief that the horizon is a classical region and should not experience significant quantum corrections [22, 23]. To alleviate the aforementioned issues, several authors have recently proposed the generalized  $\mu_0$ -scheme [36–39]. In addition, the quantum collapsing model introduced in [40] offers an additional approach to mitigating these problems.

Recently, a novel and intriguing uniparametric polymerisation scheme<sup>1</sup> has been proposed to obtain a spherically symmetric LQG-BH [42, 43]. For the sake of convenience, we will refer this novel polymerisation scheme as the Alonso-Bardaji-Brizuela-Vera (ABBV) scheme, and thus this novel LQG-BH model as the ABBV BH. Like many other LQG-BH models, the quantum gravity effects introduced in this novel ABBV BH model removes the classical singularity. A more significant advancement is that in this model of [42, 43], the modified constraint algebra exhibits closure. Thus, the system offers a reliable and clear geometric representation that remains consistent, covariant, and unambiguous, regardless of the gauge choice on the phase space<sup>2</sup>. A multitude of research have investigated various aspects of this model. The analysis of QNMs related to this BH is detailed in [45–47]. Solar system test constraints are discussed in [48]. The potential detection of quantum gravity effects

---

<sup>1</sup> The phase space regularization technique employed in LQG is also known as polymerization [41].

<sup>2</sup> More recently, the topic of BHs and covariance in effective quantum gravity has been discussed in [44]. In this work, two LQG-BH solutions with general covariance were constructed.

using eccentric extreme mass-ratio inspirals (EMRIs) is explored in [49], similar work for a LQG inspired rotating black hole can be found in [50]. Gravitational lensing and optical characteristics are studied in [51–53]. Furthermore, following similar procedures as [42, 43], the authors in [54] extend the ABBV model to include the charged case, showing that the Cauchy horizon lies within the transition surface. Additionally, they demonstrate the existence of limiting states with zero surface gravity. Our research aims to explore the characteristics of the quasinormal modes (QNMs) of a probing scalar field over the charged ABBV BH.

During the late stages of an BH’s formation, known as ringdown emission, the gravitational waves (GWs) are primarily characterized by a superposition of exponentially damped sinusoids, i.e., QNMs. These modes have frequencies and damping times that are only determined by the BH’s intrinsic parameters, including its mass and angular momentum. Recent studies have demonstrated that even minor modifications to the BH background geometry can leave a noticeable imprint on the QNM spectra [45, 55–68], which provide a test of the no-hair theorem, alternatives to GR, and quantum gravity effect. The main findings are summarized as follows. First, in some effective quantum gravity model, a non-monotonic behavior of the quasinormal frequencies (QNFs) as a function of the corrected parameters is observed as the extremal BH is approached [45, 58, 59, 65, 66]. This phenomenon is typically observed in modes with the lowest angular quantum number, but as the angular quantum number increases, the non-monotonic behavior gradually disappears. This suggests that the influence of the angular quantum number begins to dominate over the effects of quantum gravity [45, 58, 59, 65, 66]. Additionally, an oscillatory pattern in the overtones as a function of the corrected parameter is detected as the extremal BH is approached [45, 58, 59, 65]. Both the non-monotonic behavior in the fundamental modes and the oscillatory pattern in the overtones may be linked to the extremal BH. The most significant finding is the overtone outburst, indicating that even a minor change in the BH background geometry results in a sudden, significant change in the overtones [45, 55–65]. The most significant finding is the overtone outburst, indicating that even a minor change in the BH background geometry results in a sudden, significant change in the overtones [45, 55–65, 67]. Notably, these studies have demonstrated a close connection between the properties of the QNFs and the small changes of the geometric structure surrounding the event horizon of a BH. This implies that investigating the overtones offers an opportunity to explore the changes in the structure of

the event horizon.

Without a doubt, quantum gravity effects induce minor changes in the effective background geometries, leaving noticeable imprints on the QNFs. Several pioneering works have explored this direction [45, 58, 59, 65, 66]. In this paper, we investigate the QNMs of a probe scalar field in the context of a charged ABBV BH. Our primary focus is on the (in)stability of this charged ABBV BH under scalar field perturbations, and main focus is on how both quantum gravity corrections and the charge influence the characteristics of the QNFs. The structure of our paper is as follows. In Section II, we provide a brief review of the charged ABBV BH and the dynamics of the scalar field. Section III presents a systematic study of the properties of QNMs. Finally, conclusions and further discussions are given in Section IV.

## II. SCALAR FIELD OVER THE CHARGED ABBV BLACK HOLE

In this section, we firstly present a brief overview of the charged ABBV BH. Following this, we derive the equations of motion (EOM) for a probe scalar field and discuss the properties of the scalar field's effective potential.

We start with the following effective LQG corrected Hamiltonian [54]:

$$H_{\text{eff}} = -\frac{1}{2G\gamma\sqrt{1+\gamma^2\delta_b^2}} \left[ \left( \frac{\sin(\delta_b b)}{\delta_b} + \frac{\gamma^2\delta_b}{\sin(\delta_b b)} - \frac{\gamma^2\delta_b Q^2}{\sin(\delta_b b)p_c} \right) p_b + 2cp_c \cos(\delta_b b) \right]. \quad (1)$$

Here,  $b$ ,  $p_b$ ,  $c$  and  $p_c$  are the conjugate variables satisfying the Poisson brackets as  $\{b, p_b\} = G\gamma$  and  $\{c, p_c\} = 2G\gamma$ . Additionally,  $Q$  is a constant associated with the charge of the BH,  $\gamma$  is the Immirzi parameter, and  $\delta_b$  is the polymerization parameter. The classical limit is obtained by taking  $\delta_b \rightarrow 0$ .

The dynamical equations can be derived from the above effective LQG corrected Hamiltonian. Solving the obtained equations yields the following static metric:

$$ds^2 = -f(r)d\tau^2 + \frac{1}{\left(1 - \frac{r_0}{m}g(r)\right)f(r)}dr^2 + r^2d\Omega^2. \quad (2)$$

The functions  $f(r)$  and  $g(r)$  in the above equation are defined as follows, respectively:

$$f(r) = 1 - \frac{2m}{r} + \frac{Q^2}{r^2}, \quad (3)$$

$$g(r) = \frac{\frac{2m}{r} - \frac{Q^2}{r^2}}{1 + \sqrt{1 - \frac{b_0^2 Q^2}{(b_0^2 - 1)m^2}}}, \quad (4)$$

where  $b_0$  is defined as  $b_0 \equiv \sqrt{1 + \gamma^2 \delta_b^2}$ . The constant of motion  $m$  is associated with the Komar mass at spatial infinity [43, 54]. This BH geometry is asymptotically flat at infinity and its horizons are located at

$$r_h^\pm = m \left( 1 \pm \sqrt{1 - \frac{Q^2}{m^2}} \right). \quad (5)$$

It is noted that the horizons of this charged ABBV BH are the same as those of the Reissner-Nordström (RN) BH.

With the introduction of LQG gravity effects, the spacetime singularity is replaced by a transition surface, also known as the bounce, which connects a BH to a white hole (WH). The bounce radius  $r_0$  is given by [54]

$$r_0 = \frac{(b_0^2 - 1)}{b_0^2} m \left( 1 + \sqrt{1 - \frac{b_0^2 Q^2}{(b_0^2 - 1) m^2}} \right), \quad (6)$$

with

$$|Q| \leq m \frac{\sqrt{b_0^2 - 1}}{b_0}. \quad (7)$$

It is found that the bounce radius  $r_0$  always remains hidden within the Cauchy horizon, satisfying the inequality  $r_h^- < r_0 < r_h^+$  [54].

Next, we study how this charged ABBV BH responds to perturbations induced by a probing massless scalar field  $\Psi$ . The dynamics of the scalar field are governed by the Klein-Gordon (KG) equation:

$$\frac{1}{\sqrt{-g}} \partial_\nu (g^{\mu\nu} \sqrt{-g} \partial_\mu \Psi) = 0, \quad (8)$$

where  $g_{\mu\nu}$  denotes the background metric. We will investigate this issue using frequency domain analysis. Due to the spherical symmetry of the spacetime being studied, we will employ spherical harmonics to separate variables for the perturbation field  $\Psi$ . Consequently, the perturbation field  $\Psi$  can be expressed as:

$$\Psi(t, r, \theta, \varphi) = \sum_{l,m} Y_{l,m}(\theta, \varphi) \frac{\psi_{l,m}(r)}{r} e^{-i\omega t}. \quad (9)$$

Here,  $Y_{l,m}(\theta, \varphi)$  represents the spherical harmonics, where  $l$  and  $m$  are the multipole and azimuthal quantum numbers, respectively. The KG equation (8) can then be reformulated into a Schrödinger-like form:

$$\frac{\partial^2 \psi}{\partial r_*^2} + (\omega^2 - V) \psi = 0. \quad (10)$$

Here,  $r_*$  represents the tortoise coordinate, determined by the following relation:

$$\frac{dr_*}{dr} = \left(1 - \frac{2m}{r} + \frac{Q^2}{r^2}\right)^{-1} \sqrt{\left(1 - \frac{r_0}{m}g(r)\right)^{-1}}. \quad (11)$$

The effective potential  $V$  in the wave equation (10) is given as follows:

$$V = f(r)\frac{l(l+1)}{r^2} + \frac{f(r)[2(m - r_0g(r))f'(r) - r_0f(r)g'(r)]}{2mr}. \quad (12)$$

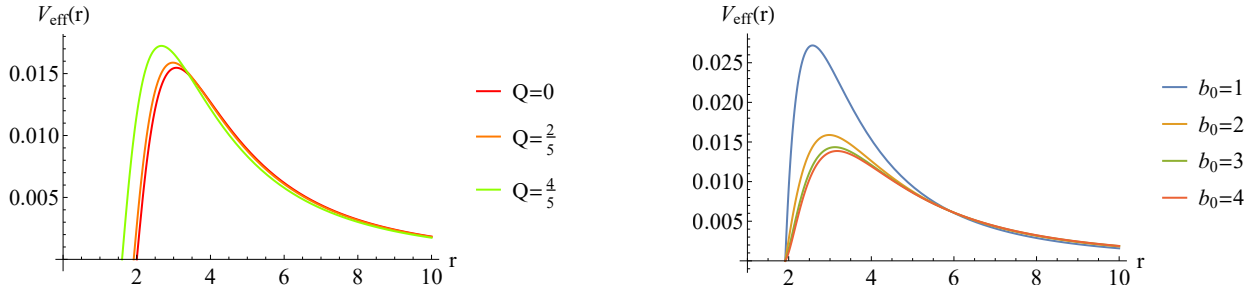


FIG. 1: The effective potential as a function  $r$  with  $l = 0$ , while considering various values for both the quantum parameter  $b_0$  and the charge  $Q$ . In the left panel, we fix the quantum parameter  $b_0 = 2$ , and then take the charge as  $Q = 0, \frac{2}{5}, \frac{4}{5}$ . Conversely, in the right panel, we set  $Q = \frac{2}{5}$ , and then the quantum parameter as  $b_0 = 1, 2, 3, 4$ .

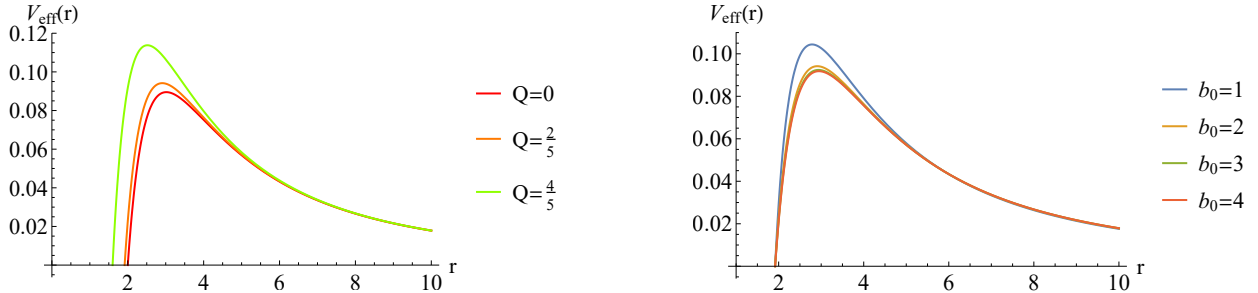


FIG. 2: The effective potential as a function  $r$  with  $l = 1$ , while considering various values for both the quantum parameter  $b_0$  and the charge  $Q$ . In the left panel, we fix the quantum parameter  $b_0 = 2$ , and then take the charge as  $Q = 0, \frac{2}{5}, \frac{4}{5}$ . Conversely, in the right panel, we set  $Q = \frac{2}{5}$ , and then take the quantum parameter as  $b_0 = 1, 2, 3, 4$ .

The above effective potential  $V$  is composed of two parts. The first term is the centrifugal potential, associated with the multipole quantum number  $l$ . The centrifugal potential prevents the wave from approaching the center, forming a barrier in regions farther away from it. The second term is the gravitational potential, related to the gravitational field or

the geometry of spacetime, which typically introduces additional attraction or barriers, influencing the wave’s decay characteristics. Notably, the quantum parameter  $b_0$  appears only in the second term, making the effects of quantum gravity most significant when  $l = 0$ . As  $l$  increases, the influence of the angular quantum number tends to overshadow the quantum gravity effects—a phenomenon observed in our previous work [45, 59, 65, 66]. Therefore, to better explore the effects of quantum gravity and charge  $Q$ , we focus primarily on the  $l = 0$  case and then briefly discuss the  $l = 1$  case.

Fig.1 and Fig.2 illustrate the effective potential  $V$  as a function of  $r$  for varying  $Q$  and  $b_0$  in the case of  $l = 0$  and  $l = 1$ , respectively<sup>3</sup>. The effective potential remains positive throughout, indicating the stability of the charged ABBV BH under scalar perturbations. Moreover, it is observed that the charge parameter  $Q$  and the quantum parameter  $b_0$  predominantly affect the behaviors of the effective potential near the horizon. It is a significant factor in inducing the so-called overtone’s outburst, as will be demonstrated below.

Before proceeding, we provide a qualitative analysis of the properties of the effective potential  $V_{eff}$  as they relate to the characteristics of the QNMs studied below. We first examine the case with fixed  $b_0$  (see the left plots in Fig.1 and Fig.2). From these plots, it is evident that the relative change for  $Q = \frac{2}{5}$  or  $Q = \frac{4}{5}$  (relative to  $Q = 0$ ) is larger for  $l = 1$  than for  $l = 0$ . This arises from the inclusion of the charge parameter in the centrifugal potential, where the increase in  $l$  results in a combined effect of  $l$  and  $Q$ , which induces such significant deviations. Next, we consider the case with the charge parameter  $Q$  fixed (see the right plots in Fig.1 and Fig.2). Compared to the case of  $b_0 = 1$ , the relative change with  $b_0 > 1$  is more pronounced for  $l = 0$  than for  $l = 1$ . This is because, as  $l$  increases, the influence of the angular quantum number tends to overshadow the effects of quantum gravity.

### III. QUASINORMAL MODES

In this section, we study the properties of QNMs arising from scalar field perturbations in the context of charged ABBV BH. The QNMs are obtained by solving an eigenvalue problem under specific boundary conditions: the wave function must represent a purely

---

<sup>3</sup> Unless otherwise specified, we will set  $m = 1$  throughout this paper.



outgoing wave at spatial infinity ( $r_* \rightarrow +\infty$ ) and a purely ingoing wave at the event horizon ( $r_* \rightarrow -\infty$ ). Mathematically, this is expressed as:

$$\psi \sim e^{\pm i\omega r_*}, \quad r_* \rightarrow \pm\infty. \quad (13)$$

These boundary conditions reflect the black hole's response to a transient perturbation, capturing the dynamics after the perturbing source has dissipated [69–71].

A variety of methods have been developed to calculate QNMs, such as the WKB method [72–77], the asymptotic iteration method (AIM) [78–80], the Horowitz-Hubeny method [81], the continued fraction method (CFM) [82], and the pseudo-spectral method (PSM) [83, 84]. In this study, we utilize the PSM to calculate the QNM spectra, given its effectiveness as a robust numerical tool [45, 58, 59, 65, 66, 83–90], especially in determining overtones [45, 59, 65].

To determine the QNM spectra using the PSM, two key steps are essential: first, working in Eddington-Finkelstein coordinates; second, discretizing the differential equations and solve the resulting generalized eigenvalue problem. The choice of Eddington-Finkelstein coordinates simplifies the boundary condition setup. To this end, we introduce the following transformations:

$$r \rightarrow \frac{r_h}{u}, \quad \text{and} \quad \Psi = e^{i\omega r_*(u)} \psi. \quad (14)$$

These transformations allow us to impose only the outgoing boundary condition at infinity. Note that, to simplify notation, we will henceforth abbreviate the outer event horizon  $r_h^+$  as  $r_h$ . With the above considerations, the wave equation (11) is transformed into:

$$\alpha_0 \psi'' + \beta_0 \psi' + \gamma_0 \psi = 0, \quad (15)$$

where  $\alpha_0$ ,  $\beta_0$ , and  $\gamma_0$  are respectively given by:

$$\begin{aligned} \alpha_0 = & 2ib_0^2 u^2 [-mu + b_0^2 (r_h + 3mu)] \omega (m - r_0 g(u)) f'(u) - ib_0^2 r_0 u^2 (-mu + b_0^2 r_h + 3b_0^2 mu) g'(u) \\ & + b_0^2 \sqrt{m} \left\{ b_0^2 (l^2 + l) \sqrt{m} u^2 + [4mr_h u \omega^2 - 2r_h \omega (-iu + 2r_h \omega + 6mu\omega)] \sqrt{m - r_0 g(u)} \right\} \\ & + \{ 2m^2 u [2mu\omega + b_0^2 (-4r_h \omega + iu - 12mu\omega)] + b_0^4 [2r_h^2 \omega - u (2r_h + 3mu) (i - 6m\omega)] \} \\ & (\omega f(u) - 2r_0 g(u)), \end{aligned} \quad (16)$$

$$\begin{aligned} \beta_0 = & ib_0^2 u^2 f(u) [-8(m - r_0 \omega g(u)) (-mu + b_0^2 r_h + 3b_0^2 mu) \omega + ib_0^2 r_0 u^2 g'(u)] \\ & + 2b_0^4 u^2 \left[ 2i\sqrt{m} r_h \omega \sqrt{m - r_0 g(u)} + u^2 (m - r_0 g(u)) f'(u) \right], \end{aligned} \quad (17)$$

$$\gamma_0 = 2b_0^4 u^2 f(u) (m - r_0 g(u)). \quad (18)$$

Next, we discretize the continuous variables using a set of Chebyshev grids and express the functions in terms of Lagrange cardinal functions. The Chebyshev grid points and the Lagrange cardinal functions are defined as follows:

$$x_i = \cos\left(\frac{i}{N}\pi\right), \quad (19)$$

$$C_j(x) = \prod_{i=0, i \neq j}^N \frac{x - x_i}{x_j - x_i}, \quad i = 0, \dots, N. \quad (20)$$

Following these operations, the wave equation is reduced to a generalized eigenvalue problem of the form:

$$(M_0 + \omega M_1) \psi = 0, \quad (21)$$

where  $M_i (i = 0, 1)$  represents a linear combination of the derivative matrices. The QNFs are then determined by solving this generalized eigenvalue equation.

### A. Fundamental modes

In this subsection, we focus solely on the case of  $l = 0$ , where only the gravitational potential remains. Fig.3 illustrates the real part,  $\omega_R$ , and the imaginary part,  $\omega_I$ , of the fundamental modes as functions of the quantum parameter  $b_0$  for various values of the charge parameter  $Q$ . When  $Q$  is fixed, an increase in  $b_0$  leads to a monotonic decrease in  $\omega_R$  and a monotonic increase in  $\omega_I$ . This behavior is consistent with the uncharged case (the black line for  $Q = 0$  and also see Ref.[45]). These observations suggest that the LQG effect reduces the oscillation behavior but simultaneously causes a slower decay of the modes, independent of the charge parameter  $Q$ .

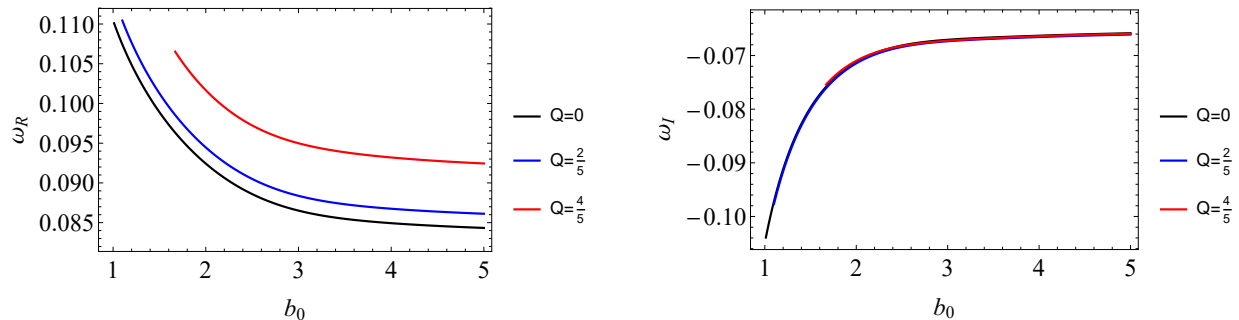


FIG. 3: QNFs of fundamental modes are presented as a function of the quantum parameter  $b_0$  for  $l = 0$ , while considering various values of the charge, specifically  $Q = 0, \frac{2}{5}, \frac{4}{5}$ .

In Fig.4, we fix the quantum parameter  $b_0$  and investigate how the fundamental modes change with  $Q$ . When  $b_0 \neq 1$ , the real part of the frequency,  $\omega_R$ , shows a monotonic increase as  $Q$  increases (left plot in Fig.4), whereas the imaginary part,  $\omega_I$ , remains nearly constant across a broad range of  $Q$  (see the right plots in Fig.4). However, for large values of  $Q$ ,  $\omega_I$  shows a slight increase. These findings suggest that the charge  $Q$  in this model enhances the oscillatory behavior while having minimal effect on the decay of the modes.

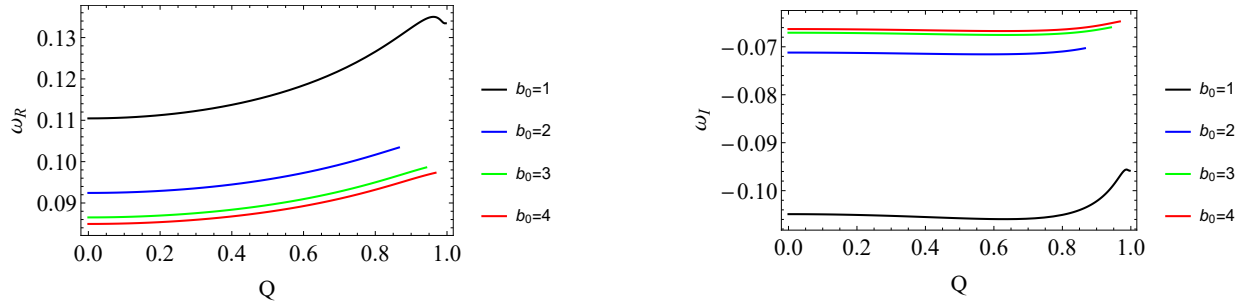


FIG. 4: QNFs of fundamental modes are presented as a function of the charge  $Q$  for  $l = 0$ , while considering various values of the quantum parameter, specifically  $b_0 = 1, 2, 3, 4$ .

Different from the previous effective quantum gravity models [45, 58, 59, 65, 66], we do not observe non-monotonic behavior of the QNFs with respect to either the quantum parameter  $b_0$  or the charge parameter  $Q$ . However, it is worth noting that when  $b_0 = 1$  corresponding to the RN scenario, both  $\omega_R$  and  $\omega_I$  as functions of  $Q$  display non-monotonic behavior as the extremal BH is approached, i.e., as  $Q$  tends to 1 (see the black line in Fig.4). Therefore, concerning non-monotonic behaviors,  $b_0$  and  $Q$  play mutually inhibiting roles.

## B. Overtones

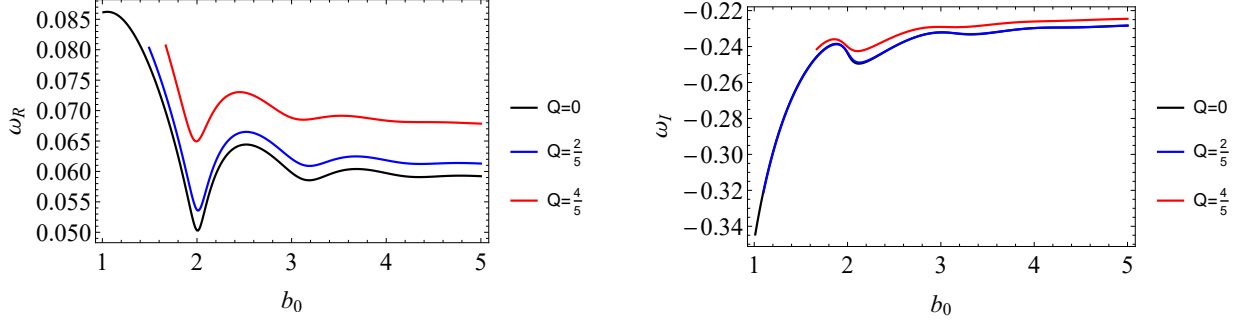


FIG. 5: QNFs of the first overtone ( $n = 1$ ) with  $l = 0$  are presented as a function of the quantum parameter  $b_0$  for the values of the charge  $Q = 0, \frac{2}{5}, \frac{4}{5}$ . The left and right panels show the real and imaginary parts, respectively.

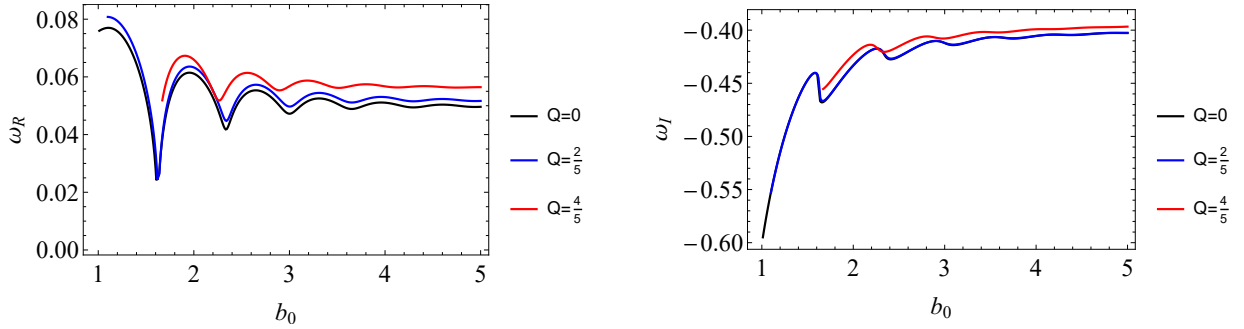


FIG. 6: QNFs of the second overtone ( $n = 2$ ) with  $l = 0$  are presented as a function of the quantum parameter  $b_0$  for the values of the charge  $Q = 0, \frac{2}{5}, \frac{4}{5}$ . The left and right panels show the real and imaginary parts, respectively.

In this subsection, we proceed to study the properties of the overtones, focusing exclusively on the case of  $l = 0$ . Fig.5 and Fig.6 show the QNFs as functions of the quantum parameter  $b_0$  for various values of  $Q$ , corresponding to the first two overtones (Fig.5 for  $n = 1$  and Fig.6 for  $n = 2$ , respectively). It is evident that the quantum gravity effects trigger the outburst of overtones, resulting in noticeable changes in the QNFs compared to those of Schwarzschild or RN BHs. This phenomenon has been widely observed in the modified gravity theory and effective quantum gravity models [45, 55–65]. Following the initial outburst of overtones, we observe an oscillatory behavior. This oscillation gradually becomes weak as the quantum parameter  $b_0$  increases. This pattern has been observed in

RN-BH [91, 92] and other effective quantum gravity corrected BH [45, 59, 65] and is likely associate with the extremal effect.

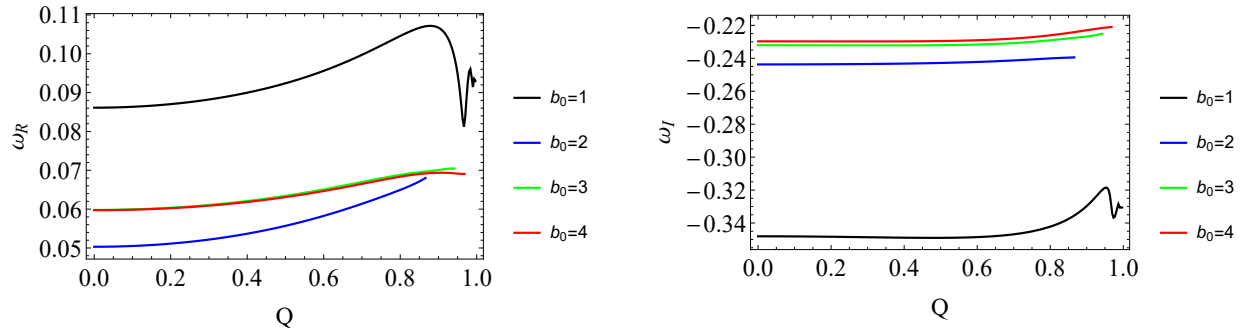


FIG. 7: QNFs of the first overtone ( $n = 1$ ) with  $l = 0$  are presented as a function of the charge  $Q$  for different quantum parameters  $b_0 = 1, 2, 3, 4$ . The left and right panels show the real and imaginary parts, respectively.

As expected, with increasing  $n$ , the overtone outburst becomes more pronounced, with smaller quantum parameters capable of triggering this outburst. For fixed  $n$ , the oscillatory behavior remains consistent across different charge parameters  $Q$ . Additionally, as  $n$  increases, the oscillations become stronger. On the other hand, as  $Q$  increases, both the strength of the overtone outburst and the oscillation become weak, suggesting that the charge does not enhance either the overtone outburst or the oscillatory behavior.

We now study the behavior of the QNFs as functions of  $Q$  with a fixed  $b_0$  (see Fig.7 and Fig.8). In the case where  $b_0 = 1$ , corresponding to the RN-BH, an overtone outburst with a distinct oscillatory pattern is observed (Fig.7). As the overtone number  $n$  increases, both the intensity of the overtone outburst and the prominence of the oscillations become more pronounced. Nevertheless, upon activation of the quantum parameter  $b_0$  ( $b_0 > 1$ ), the overtone outburst vanishes for the first overtone within the allowed range of  $Q$  (see Fig.7). For the second overtone, once the quantum parameter  $b_0$  is activated, the overtone outburst degenerates into non-monotonic behavior (see Fig.8). In conclusion, the charge  $Q$  and the quantum parameter  $b_0$  appear to exert mutually suppressive effects on the overtone outburst. The analogous effect on non-monotonic behaviors has also been noted in the preceding subsection.

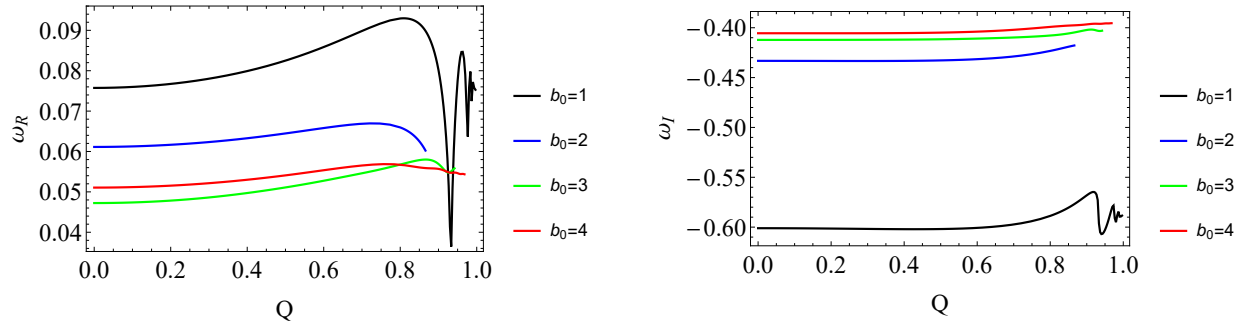


FIG. 8: QNFs of the second overtone ( $n = 2$ ) with  $l = 0$  are presented as a function of the charge  $Q$  for different quantum parameters  $b_0 = 1, 2, 3, 4$ . The left and right panels show the real and imaginary parts, respectively.

### C. QNFs with $l = 1$

In this subsection, we turn on the multipole quantum number  $l$  and analyze the properties of the QNFs. Fig.9 presents the QNFs with  $l = 1$  as a function of  $b_0$  for  $Q = \frac{2}{5}$ . For the fundamental mode ( $n = 0$ ), increasing  $b_0$  results in a monotonic decrease in  $\omega_R$  and a monotonic increase in  $\omega_I$ , consistent with the  $l = 0$  case. For the first two overtones,  $\omega_R$  exhibits non-monotonic behavior as a function of  $b_0$ , in contrast to the overtone outburst observed in the case of  $l = 0$ . This is likely due to the activation of the centrifugal potential for non-zero  $l$  is non-zero, which suppresses the gravitational potential and, consequently, the quantum gravity effect. As discussed in the introduction and also in [59, 65], the non-monotonic behavior in  $\omega_R$  is also the manifestation of the quantum gravity effect. When the charge parameter  $Q$  is increased (see Fig.10 for  $Q = \frac{2}{5}$ ), the non-monotonic behavior in  $\omega_R$  disappears, likely because the centrifugal potential's influence strengthens, further suppressing the quantum gravity effect.

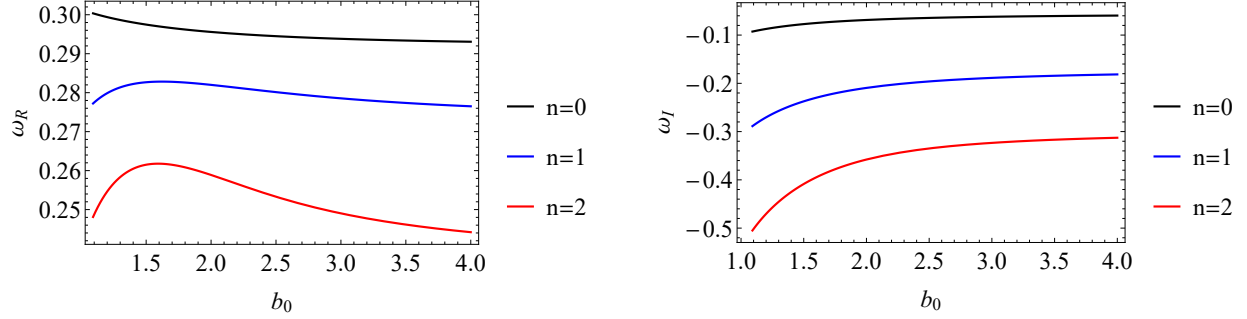


FIG. 9: QNFs of fundamental mode and the first two overtones with  $l = 1$  are presented as functions of the quantum parameter  $b_0$  for  $Q = \frac{2}{5}$ . The left and right panels show the real and imaginary parts, respectively.

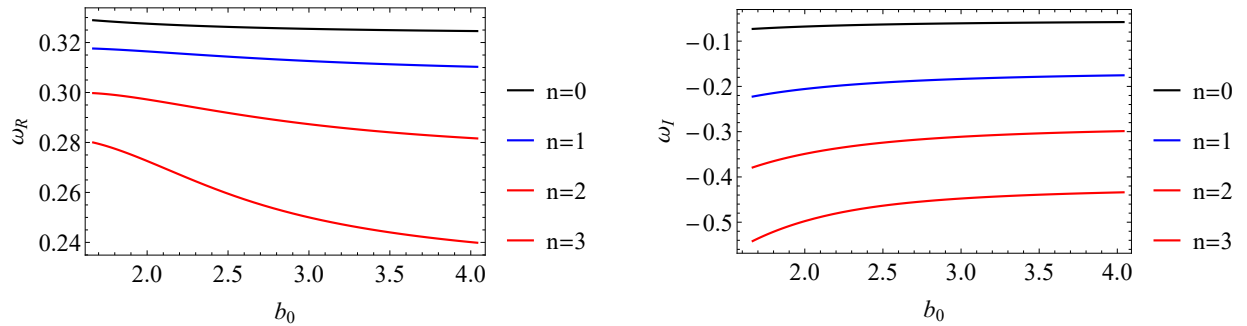


FIG. 10: QNFs of fundamental mode and the first three overtones with  $l = 1$  are presented as functions of the quantum parameter  $b_0$  for  $Q = \frac{4}{5}$ . The left and right panels show the real and imaginary parts, respectively.

#### IV. CONCLUSIONS AND DISCUSSIONS

In this paper, we have systematically analyzed the properties of the QNMs of the scalar field around a charged ABBV BH. The black hole is characterized by two parameters: the quantum parameter  $b_0$ , originating from LQG corrections, and the charge parameter  $Q$ . The quantum parameter  $b_0$  modifies only the gravitational potential, while the charge parameter  $Q$  influences both the centrifugal and gravitational potentials. Our analysis focused on two scenarios: first, the case of  $l = 0$ , where only the gravitational potential is involved, and second, when the multipole quantum number  $l$  is non-zero, introducing the centrifugal potential.

For the case of  $l = 0$ , our results demonstrate that quantum gravity effects significantly alter the behavior of QNMs. We observed that quantum gravity induces an overtone outburst

in the QNFs, producing substantial deviations compared to the Schwarzschild or RN BHs. With increasing  $n$ , the overtone outburst becomes more pronounced, with smaller quantum parameters capable of triggering this outburst, suggesting a sensitive dependence of QNFs on LQG corrections. This outburst is accompanied by an oscillatory pattern that intensifies with increasing overtone number  $n$ . When fixing  $b_0$  and varying the charge parameter  $Q$ , the overtone outburst disappears within the allowed range of  $Q$ .

When the multipole quantum number  $l$  is turned on (i.e.,  $l > 0$ ), no overtone outburst is observed. This can be attributed to the centrifugal potential, which suppresses the quantum gravity effect. However, we still observe non-monotonic behavior in the first two overtones as a function of  $b_0$ , suggesting that subtle quantum gravity effects persist. The disappearance of this non-monotonic behavior with increasing charge  $Q$  further supports the suppressive role of the centrifugal potential, in agreement with our observations for  $l = 0$ .

Looking forward, it would be interesting to extend this analysis to other types of perturbative fields, such as electromagnetic or gravitational perturbations, and to explore more general models with different types of quantum gravity corrections. Further, a deeper understanding of the physical mechanism behind the overtone outburst and the role of different parameters in governing this phenomenon could shed light on new physics beyond GR.

## Acknowledgments

This work is supported by National Key R&D Program of China (No. 2020YFC2201400), the Natural Science Foundation of China under Grants No. 12375055 and 12347159.

- 
- [1] C. Rovelli, *Quantum Gravity*, Cambridge University Press, Cambridge, UK (2004).
  - [2] T. Thiemann, *Modern canonical quantum general relativity*, [gr-qc/0110034](#).
  - [3] A. Ashtekar and J. Lewandowski, *Background independent quantum gravity: A Status report*, Class. Quant. Grav. **21** (2004) R53, [[gr-qc/0404018](#)].
  - [4] M. Han, W. Huang, and Y. Ma, *Fundamental structure of loop quantum gravity*, Int. J. Mod. Phys. D **16** (2007) 1397–1474, [[gr-qc/0509064](#)].
  - [5] M. Bojowald, *Absence of singularity in loop quantum cosmology*, Phys. Rev. Lett. **86** (2001) 5227–5230, [[gr-qc/0102069](#)].



- [6] A. Ashtekar, T. Pawłowski, and P. Singh, *Quantum nature of the big bang*, Phys. Rev. Lett. **96** (2006) 141301, [[gr-qc/0602086](#)].
- [7] A. Ashtekar, T. Pawłowski, and P. Singh, *Quantum Nature of the Big Bang: An Analytical and Numerical Investigation. I.*, Phys. Rev. D **73** (2006) 124038, [[gr-qc/0604013](#)].
- [8] A. Ashtekar, T. Pawłowski, and P. Singh, *Quantum Nature of the Big Bang: Improved dynamics*, Phys. Rev. D **74** (2006) 084003, [[gr-qc/0607039](#)].
- [9] A. Ashtekar, M. Bojowald, and J. Lewandowski, *Mathematical structure of loop quantum cosmology*, Adv. Theor. Math. Phys. **7** (2003), no. 2 233–268, [[gr-qc/0304074](#)].
- [10] M. Bojowald, *Loop quantum cosmology*, Living Rev. Rel. **8** (2005) 11, [[gr-qc/0601085](#)].
- [11] A. Ashtekar and P. Singh, *Loop Quantum Cosmology: A Status Report*, Class. Quant. Grav. **28** (2011) 213001, [[arXiv:1108.0893](#)].
- [12] E. Wilson-Ewing, *Testing loop quantum cosmology*, Comptes Rendus Physique **18** (2017) 207–225, [[arXiv:1612.04551](#)].
- [13] M. Bojowald, G. Date, and K. Vandersloot, *Homogeneous loop quantum cosmology: The Role of the spin connection*, Class. Quant. Grav. **21** (2004) 1253–1278, [[gr-qc/0311004](#)].
- [14] P. Singh and A. Toporensky, *Big crunch avoidance in  $K=1$  semiclassical loop quantum cosmology*, Phys. Rev. D **69** (2004) 104008, [[gr-qc/0312110](#)].
- [15] G. V. Vereshchagin, *Qualitative approach to semi-classical loop quantum cosmology*, JCAP **07** (2004) 013, [[gr-qc/0406108](#)].
- [16] G. Date, *Absence of the Kasner singularity in the effective dynamics from loop quantum cosmology*, Phys. Rev. D **71** (2005) 127502, [[gr-qc/0505002](#)].
- [17] G. Date and G. M. Hossain, *Genericity of big bounce in isotropic loop quantum cosmology*, Phys. Rev. Lett. **94** (2005) 011302, [[gr-qc/0407074](#)].
- [18] R. Goswami, P. S. Joshi, and P. Singh, *Quantum evaporation of a naked singularity*, Phys. Rev. Lett. **96** (2006) 031302, [[gr-qc/0506129](#)].
- [19] M. Bojowald, *The Early universe in loop quantum cosmology*, J. Phys. Conf. Ser. **24** (2005) 77–86, [[gr-qc/0503020](#)].
- [20] T. Stachowiak and M. Szydlowski, *Exact solutions in bouncing cosmology*, Phys. Lett. B **646** (2007) 209–214, [[gr-qc/0610121](#)].
- [21] A. Ashtekar and M. Bojowald, *Quantum geometry and the Schwarzschild singularity*, Class. Quant. Grav. **23** (2006) 391–411, [[gr-qc/0509075](#)].

- [22] C. G. Boehmer and K. Vandersloot, *Loop Quantum Dynamics of the Schwarzschild Interior*, Phys. Rev. D **76** (2007) 104030, [[arXiv:0709.2129](#)].
- [23] D.-W. Chiou, *Phenomenological loop quantum geometry of the Schwarzschild black hole*, Phys. Rev. D **78** (2008) 064040, [[arXiv:0807.0665](#)].
- [24] A. Perez, *Black Holes in Loop Quantum Gravity*, Rept. Prog. Phys. **80** (2017), no. 12 126901, [[arXiv:1703.09149](#)].
- [25] X. Zhang, *Loop Quantum Black Hole*, Universe **9** (2023), no. 7 313, [[arXiv:2308.10184](#)].
- [26] L. Modesto, *Loop quantum black hole*, Class. Quant. Grav. **23** (2006) 5587–5602, [[gr-qc/0509078](#)].
- [27] L. Modesto, *Semiclassical loop quantum black hole*, Int. J. Theor. Phys. **49** (2010) 1649–1683, [[arXiv:0811.2196](#)].
- [28] M. Campiglia, R. Gambini, and J. Pullin, *Loop quantization of spherically symmetric midi-superspaces*, Class. Quant. Grav. **24** (2007) 3649–3672, [[gr-qc/0703135](#)].
- [29] M. Bojowald and S. Brahma, *Signature change in two-dimensional black-hole models of loop quantum gravity*, Phys. Rev. D **98** (2018), no. 2 026012, [[arXiv:1610.08850](#)].
- [30] A. Joe and P. Singh, *Kantowski-Sachs spacetime in loop quantum cosmology: bounds on expansion and shear scalars and the viability of quantization prescriptions*, Class. Quant. Grav. **32** (2015), no. 1 015009, [[arXiv:1407.2428](#)].
- [31] D.-W. Chiou, *Phenomenological dynamics of loop quantum cosmology in Kantowski-Sachs spacetime*, Phys. Rev. D **78** (2008) 044019, [[arXiv:0803.3659](#)].
- [32] R. Gambini, J. Olmedo, and J. Pullin, *Spherically symmetric loop quantum gravity: analysis of improved dynamics*, Class. Quant. Grav. **37** (2020), no. 20 205012, [[arXiv:2006.01513](#)].
- [33] J. G. Kelly, R. Santacruz, and E. Wilson-Ewing, *Effective loop quantum gravity framework for vacuum spherically symmetric spacetimes*, Phys. Rev. D **102** (2020), no. 10 106024, [[arXiv:2006.09302](#)].
- [34] V. Husain, J. G. Kelly, R. Santacruz, and E. Wilson-Ewing, *Fate of quantum black holes*, Phys. Rev. D **106** (2022), no. 2 024014, [[arXiv:2203.04238](#)].
- [35] M. Han and H. Liu, *Covariant  $\bar{\mu}$ -scheme effective dynamics, mimetic gravity, and non-singular black holes: Applications to spherical symmetric quantum gravity and CGHS model*, [[arXiv:2212.04605](#)].
- [36] A. Corichi and P. Singh, *Loop quantization of the Schwarzschild interior revisited*, Class.

- Quant. Grav. **33** (2016), no. 5 055006, [[arXiv:1506.08015](#)].
- [37] J. Olmedo, S. Saini, and P. Singh, *From black holes to white holes: a quantum gravitational, symmetric bounce*, Class. Quant. Grav. **34** (2017), no. 22 225011, [[arXiv:1707.07333](#)].
- [38] A. Ashtekar, J. Olmedo, and P. Singh, *Quantum Transfiguration of Kruskal Black Holes*, Phys. Rev. Lett. **121** (2018), no. 24 241301, [[arXiv:1806.00648](#)].
- [39] A. Ashtekar, J. Olmedo, and P. Singh, *Quantum extension of the Kruskal spacetime*, Phys. Rev. D **98** (2018), no. 12 126003, [[arXiv:1806.02406](#)].
- [40] J. Lewandowski, Y. Ma, J. Yang, and C. Zhang, *Quantum Oppenheimer-Snyder and Swiss Cheese Models*, Phys. Rev. Lett. **130** (2023), no. 10 101501, [[arXiv:2210.02253](#)].
- [41] A. Corichi, T. Vukasinac, and J. A. Zapata, *Polymer Quantum Mechanics and its Continuum Limit*, Phys. Rev. D **76** (2007) 044016, [[arXiv:0704.0007](#)].
- [42] A. AlonsoBardaji, D. Brizuela, and R. Vera, *An effective model for the quantum Schwarzschild black hole*, Phys. Lett. B **829** (2022) 137075, [[arXiv:2112.12110](#)].
- [43] A. AlonsoBardaji, D. Brizuela, and R. Vera, *Nonsingular spherically symmetric black-hole model with holonomy corrections*, Phys. Rev. D **106** (2022), no. 2 024035, [[arXiv:2205.02098](#)].
- [44] C. Zhang, J. Lewandowski, Y. Ma, and J. Yang, *Black Holes and Covariance in Effective Quantum Gravity*, [arXiv:2407.10168](#).
- [45] G. Fu, D. Zhang, P. Liu, X.-M. Kuang, and J.-P. Wu, *Peculiar properties in quasinormal spectra from loop quantum gravity effect*, Phys. Rev. D **109** (2024), no. 2 026010, [[arXiv:2301.08421](#)].
- [46] Z. S. Moreira, H. C. D. Lima Junior, L. C. B. Crispino, and C. A. R. Herdeiro, *Quasinormal modes of a holonomy corrected Schwarzschild black hole*, Phys. Rev. D **107** (2023), no. 10 104016, [[arXiv:2302.14722](#)].
- [47] S. V. Bolokhov, *Long-lived quasinormal modes and overtones' behavior of the holonomy corrected black holes*, [arXiv:2311.05503](#).
- [48] R.-T. Chen, S. Li, L.-G. Zhu, and J.-P. Wu, *Constraints from Solar System tests on a covariant loop quantum black hole*, Phys. Rev. D **109** (2024), no. 2 024010, [[arXiv:2311.12270](#)].
- [49] G. Fu, Y. Liu, B. Wang, J.-P. Wu, and C. Zhang, *Probing Quantum Gravity Effects with Eccentric Extreme Mass-Ratio Inspirals*, [arXiv:2409.08138](#).

- [50] T. Zi and S. Kumar, *Eccentric extreme mass-ratio inspirals: A gateway to probe quantum gravity effects*, [arXiv:2409.17765](#).
- [51] A. R. Soares, C. F. S. Pereira, and R. L. L. Vitória, *Holonomy corrected Schwarzschild black hole lensing*, [arXiv:2309.05106](#).
- [52] E. L. B. Junior, F. S. N. Lobo, M. E. Rodrigues, and H. A. Vieira, *Gravitational lens effect of a holonomy corrected Schwarzschild black hole*, [arXiv:2309.02658](#).
- [53] A. E. Balali, *Quantum Schwarzschild Black Hole Optical Aspects*, [arXiv:2310.09829](#).
- [54] H. A. Borges, I. P. R. Baranov, F. C. Sobrinho, and S. Carneiro, *Remnant loop quantum black holes*, Class. Quant. Grav. **41** (2024), no. 5 05LT01, [[arXiv:2310.01560](#)].
- [55] R. A. Konoplya and A. Zhidenko, *First few overtones probe the event horizon geometry*, [arXiv:2209.00679](#).
- [56] E. Berti, V. Cardoso, and C. M. Will, *On gravitational-wave spectroscopy of massive black holes with the space interferometer LISA*, Phys. Rev. D **73** (2006) 064030, [[gr-qc/0512160](#)].
- [57] E. Berti, K. Yagi, H. Yang, and N. Yunes, *Extreme Gravity Tests with Gravitational Waves from Compact Binary Coalescences: (II) Ringdown*, Gen. Rel. Grav. **50** (2018), no. 5 49, [[arXiv:1801.03587](#)].
- [58] G. Fu, D. Zhang, P. Liu, X.-M. Kuang, Q. Pan, and J.-P. Wu, *Quasinormal modes and Hawking radiation of a charged Weyl black hole*, Phys. Rev. D **107** (2023), no. 4 044049, [[arXiv:2207.12927](#)].
- [59] H. Gong, S. Li, D. Zhang, G. Fu, and J.-P. Wu, *Quasinormal modes of quantum-corrected black holes*, [arXiv:2312.17639](#).
- [60] F. Moura and J. a. Rodrigues, *Eikonal quasinormal modes and shadow of string-corrected d-dimensional black holes*, Phys. Lett. B **819** (2021) 136407, [[arXiv:2103.09302](#)].
- [61] F. Moura and J. a. Rodrigues, *Asymptotic quasinormal modes of string-theoretical d-dimensional black holes*, JHEP **08** (2021) 078, [[arXiv:2105.02616](#)].
- [62] F. Moura and J. a. Rodrigues, *The isospectrality of asymptotic quasinormal modes of large Gauss-Bonnet d-dimensional black holes*, Nucl. Phys. B **993** (2023) 116255, [[arXiv:2206.11377](#)].
- [63] J. Lin, M. Bravo-Gaete, and X. Zhang, *Quasinormal modes, greybody factors, and thermodynamics of four dimensional AdS black holes in critical gravity*, Phys. Rev. D **109** (2024), no. 10 104039, [[arXiv:2401.02045](#)].

- [64] R. Ghosh, M. Rahman, and A. K. Mishra, *Regularized stable Kerr black hole: cosmic censorship, shadow and quasi-normal modes*, Eur. Phys. J. C **83** (2023), no. 1 91, [[arXiv:2209.12291](#)].
- [65] D. Zhang, H. Gong, G. Fu, J.-P. Wu, and Q. Pan, *Quasinormal modes of a regular black hole with sub-Planckian curvature*, Eur. Phys. J. C **84** (2024), no. 6 564, [[arXiv:2402.15085](#)].
- [66] Z. Song, H. Gong, H.-L. Li, G. Fu, L.-G. Zhu, and J.-P. Wu, *Quasinormal modes and ringdown waveform of the Frolov black hole*, [arXiv:2406.04787](#).
- [67] R. A. Konoplya and O. S. Stashko, *Probing the Effective Quantum Gravity via Quasinormal Modes and Shadows of Black Holes*, [arXiv:2408.02578](#).
- [68] O. Stashko, *Quasinormal modes and gray-body factors of regular black holes in asymptotically safe gravity*, [arXiv:2407.07892](#).
- [69] R. A. Konoplya and A. Zhidenko, *Quasinormal modes of black holes: From astrophysics to string theory*, Rev. Mod. Phys. **83** (2011) 793–836, [[arXiv:1102.4014](#)].
- [70] E. Berti, V. Cardoso, and A. O. Starinets, *Quasinormal modes of black holes and black branes*, Class. Quant. Grav. **26** (2009) 163001, [[arXiv:0905.2975](#)].
- [71] K. D. Kokkotas and B. G. Schmidt, *Quasinormal modes of stars and black holes*, Living Rev. Rel. **2** (1999) 2, [[gr-qc/9909058](#)].
- [72] V. Ferrari and B. Mashhoon, *New approach to the quasinormal modes of a black hole*, Phys. Rev. D **30** (1984) 295–304.
- [73] B. F. Schutz and C. M. Will, *BLACK HOLE NORMAL MODES: A SEMIANALYTIC APPROACH*, Astrophys. J. Lett. **291** (1985) L33–L36.
- [74] S. Iyer and C. M. Will, *Black Hole Normal Modes: A WKB Approach. 1. Foundations and Application of a Higher Order WKB Analysis of Potential Barrier Scattering*, Phys. Rev. D **35** (1987) 3621.
- [75] S. Iyer, *BLACK HOLE NORMAL MODES: A WKB APPROACH. 2. SCHWARZSCHILD BLACK HOLES*, Phys. Rev. D **35** (1987) 3632.
- [76] R. A. Konoplya, *Quasinormal behavior of the  $d$ -dimensional Schwarzschild black hole and higher order WKB approach*, Phys. Rev. D **68** (2003) 024018, [[gr-qc/0303052](#)].
- [77] J. Matyjasek and M. Opala, *Quasinormal modes of black holes. The improved semianalytic approach*, Phys. Rev. D **96** (2017), no. 2 024011, [[arXiv:1704.00361](#)].
- [78] H. Ciftci, R. L. Hall, and N. Saad, *Perturbation theory in a framework of iteration methods*,

- Phys. Lett. A **340** (2005) 388–396, [[math-ph/0504056](#)].
- [79] H. T. Cho, A. S. Cornell, J. Doukas, and W. Naylor, *Black hole quasinormal modes using the asymptotic iteration method*, Class. Quant. Grav. **27** (2010) 155004, [[arXiv:0912.2740](#)].
- [80] H. T. Cho, A. S. Cornell, J. Doukas, T. R. Huang, and W. Naylor, *A New Approach to Black Hole Quasinormal Modes: A Review of the Asymptotic Iteration Method*, Adv. Math. Phys. **2012** (2012) 281705, [[arXiv:1111.5024](#)].
- [81] G. T. Horowitz and V. E. Hubeny, *Quasinormal modes of AdS black holes and the approach to thermal equilibrium*, Phys. Rev. D **62** (2000) 024027, [[hep-th/9909056](#)].
- [82] E. W. Leaver, *An Analytic representation for the quasi normal modes of Kerr black holes*, Proc. Roy. Soc. Lond. A **402** (1985) 285–298.
- [83] J. P. Boyd, Chebyshev and Fourier spectral methods. Courier Corporation, 2001.
- [84] A. Jansen, *Overdamped modes in Schwarzschild-de Sitter and a Mathematica package for the numerical computation of quasinormal modes*, Eur. Phys. J. Plus **132** (2017), no. 12 546, [[arXiv:1709.09178](#)].
- [85] J.-P. Wu and P. Liu, *Quasi-normal modes of holographic system with Weyl correction and momentum dissipation*, Phys. Lett. B **780** (2018) 616–621, [[arXiv:1804.10897](#)].
- [86] G. Fu and J.-P. Wu, *EM Duality and Quasinormal Modes from Higher Derivatives with Homogeneous Disorder*, Adv. High Energy Phys. **2019** (2019) 5472310, [[arXiv:1812.11522](#)].
- [87] P. Liu, C. Niu, and C.-Y. Zhang, *Linear instability of charged massless scalar perturbation in regularized 4D charged Einstein-Gauss-Bonnet anti de-Sitter black holes*, Chin. Phys. C **45** (2021), no. 2 025111.
- [88] K. Destounis, R. P. Macedo, E. Berti, V. Cardoso, and J. L. Jaramillo, *Pseudospectrum of Reissner-Nordström black holes: Quasinormal mode instability and universality*, Phys. Rev. D **104** (2021), no. 8 084091, [[arXiv:2107.09673](#)].
- [89] J. L. Jaramillo, R. Panosso Macedo, and L. A. Sheikh, *Gravitational wave signatures of black hole quasi-normal mode instability*, [arXiv:2105.03451](#).
- [90] W. Xiong, P. Liu, C.-Y. Zhang, and C. Niu, *Quasi-normal modes of the Einstein-Maxwell-aether Black Hole*, [arXiv:2112.12523](#).
- [91] E. Berti and K. D. Kokkotas, *Asymptotic quasinormal modes of Reissner-Nordstrom and Kerr black holes*, Phys. Rev. D **68** (2003) 044027, [[hep-th/0303029](#)].
- [92] J. Jing and Q. Pan, *Quasinormal modes and second order thermodynamic phase transition*

for Reissner-Nordstrom black hole, Phys. Lett. B **660** (2008) 13–18, [[arXiv:0802.0043](#)].